

Gas-Phase Reactions of HONO with HNO and NH₃: an Ab Initio MO/TST StudyXin Lu,[†] Ryza N. Musin, and M. C. Lin*

Department of Chemistry, Emory University, and Cherry L. Emerson Center for Scientific Computation, Emory University, Atlanta, Georgia 30322

Received: February 4, 2000; In Final Form: March 20, 2000

The reduction of HONO by HNO and NH₃ has been investigated by means of ab initio molecular orbital and transition-state theory (TST) calculations. The main reaction channels for the HNO + *trans*-HONO (*cis*-HONO) reactions are those proceeding via five-member ring transition states, leading to the production of NO and H₂O. In the temperature range 300–1000 K, TST calculations predict an A factor of $2.25 \times 10^{10} \text{ cm}^3 \text{ mol}^{-1} \text{ s}^{-1}$ (or $3.63 \times 10^{10} \text{ cm}^3 \text{ mol}^{-1} \text{ s}^{-1}$) and an apparent activation energy of 20.9 kcal/mol (or 21.9 kcal/mol) for the HNO + *trans*-HONO (or *cis*-HONO) reaction. In the NH₃ + HONO system, the reaction NH₃ + *cis/trans*-HONO → H₂NNO + H₂O with barrier heights centering around 34 kcal/mol can occur at high temperatures. The reversible H-atom exchange reaction NH₃ + *cis*-HONO ⇌ H₂NH–O(H)NO ⇌ NH₂H + *cis*-HONO occurs readily. The calculated rate constant for the reaction at 300 K is $1.06 \times 10^6 \text{ cm}^3 \text{ mol}^{-1} \text{ s}^{-1}$, in reasonable agreement with the experimental value of $2.2 \times 10^6 \text{ cm}^3 \text{ mol}^{-1} \text{ s}^{-1}$.

I. Introduction

It has been long known that nitrous acid (HONO) is a key reactive intermediate during the course of the chemical reactions in H/N/O-containing systems.^{1–4} HONO is chemically relatively stable; it can be possibly accumulated at low temperatures.^{5,6} Over the decades, the chemistry of H/N/O systems has received much attention thanks to its significant relevance to the combustion of many nitramine propellants and to the chemistry of the polluted troposphere. Accordingly, the study of HONO reactions is of great importance to our understanding of the H/N/O chemistry pertinent to the combustion of propellants and to pollution control in the troposphere.

Recently, a systematic study of HONO reactions by ab initio molecular orbital and transition-state theory (ab initio MO/TST) calculations has been performed in our laboratory. The reactions include the direct oxidation of HNO by NO₂ to produce HONO and NO,⁶ the bimolecular decomposition of HONO,⁷ the oxidation of HONO by NO₂ and O₃, and the reduction of HONO by HNO and NH₃. In the present paper, we report our theoretical results from the latter study. The results on the oxidation of HONO by NO₂ and O₃ will be presented in a forthcoming paper.⁸

II. Computational Details

The structures of the reactants, products, intermediates, and transition states of the two title reactions have been fully optimized using the hybrid density functional B3LYP method (Becke's three-parameter nonlocal exchange functional^{9–11} with the correlation functional of Lee et al.¹²) with the 6-311G(d,p) basis set.¹³ Vibrational frequencies and zero-point energy (ZPE) corrections have been obtained at the same level of theory, and used for the subsequent TST calculations of rate constants. Each of the calculated transition states has been identified to have

one imaginary frequency. All the stationary points (transition states and adjacent local minima) along the reaction paths have been connected by using the intrinsic reaction coordinate (IRC) calculations.¹⁴ All the energies quoted and discussed in the present article include the ZPE correction.

To obtain more reliable energies, we carried out QCISD(T)/6-311G(d,p),¹⁵ restricted closed-shell and open-shell coupled cluster RCCSD(T)/6-311G(d,p),¹⁶ as well as G2M(RCC,MP2)¹⁷ calculations. The G2M(RCC,MP2) method is a modification of the Gaussian-2 (G2) approach;¹⁸ it uses B3LYP/6-311G(d,p) optimized geometries and ZPE corrections and substitutes the QCISD(T)/6-311G(d,p) calculation of the original G2 scheme by the RCCSD(T)/6-311G(d,p) calculation. The total energy in G2M(RCC,MP2) is calculated as follows:¹⁷

$$E[\text{G2M(RCC,MP2)}] = E[(\text{RCCSD(T)/6-311G(d,p)}) + \Delta E(+3\text{df},2\text{p}) + \Delta E(\text{HLC}) + \text{ZPE}]$$

where

$$\Delta E(+3\text{df},2\text{p}) = E[\text{MP2/6-311+G(3df},2\text{p)}] - E[\text{MP2/6-311G(d,p)}]$$

and the empirical "higher-level correction"(HLC) in millihartrees

$$\Delta E(\text{HLC}) = -5.25n_{\beta} - 0.19n_{\alpha}$$

where n_{α} and n_{β} are the numbers of α and β valence electrons, respectively.

All the ab initio calculations were performed using the GAUSSIAN94¹⁹ and MOLPRO96²⁰ programs.

III. Results and Discussion

HNO + HONO Reaction. So far, neither theoretical nor experimental work has been done on the HNO + HONO reaction. The previous ab initio and TST study of the bimolecular decomposition of HONO reveals that the reaction can proceed by a hydrogen transfer from one HONO to the O(H) atom of the second molecule accompanied by elimination of

* Corresponding author. E-mail: chemmcl@emory.edu.

[†] Permanent address: State Key Laboratory for Physical Chemistry of Solid Surface and Department of Chemistry, Xiamen University, Xiamen 361005, PR China.

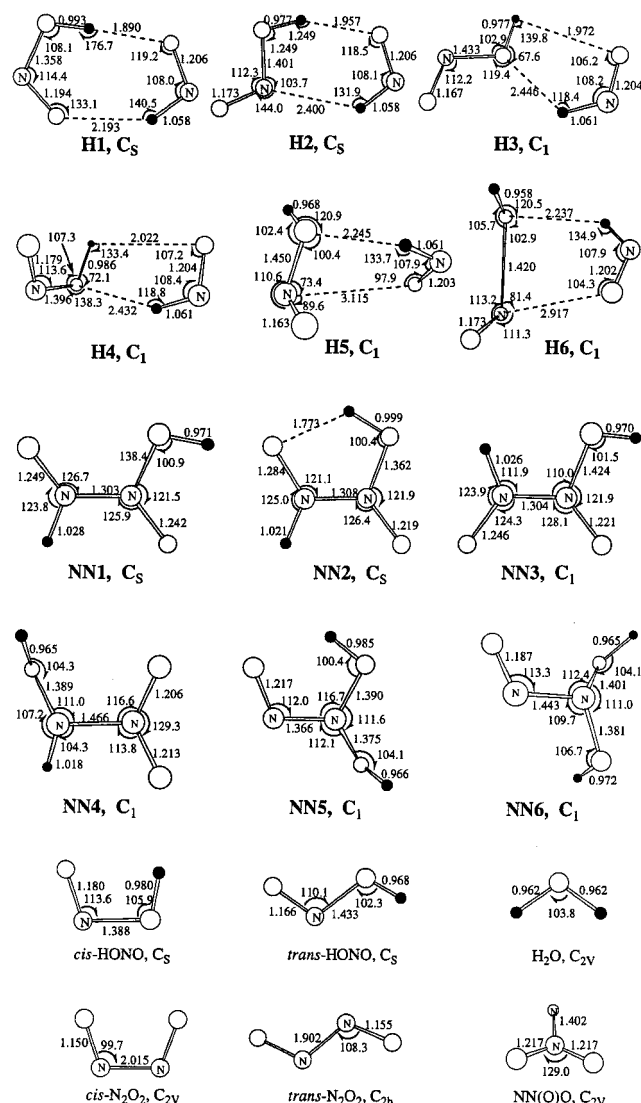
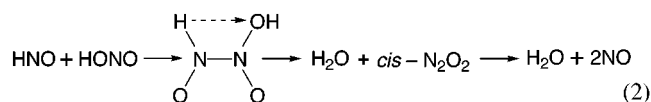


Figure 1. B3LYP/6-311G(d,p) optimized structures (bond lengths in angstroms, bond angles in degrees) of the reactants, intermediates, and products of the HNO + HONO reaction.

H_2O .⁷ It can be analogously deduced that the HNO + HONO reaction proceeds in a similar manner in that the H atom of HNO directly attacks the O(H) atom of HONO, producing H_2O and 2NO. This channel can be referred to as “direct elimination of H_2O ”, and can be expressed simply as



Another possible path of this reaction is the association/elimination process:



which proceeds via a HN(O)N(O)OH intermediate. The products of this channel are H_2O and $\text{cis-N}_2\text{O}_2$, which fragments to give 2NO readily. $\text{cis-N}_2\text{O}_2$ has been known both experimentally and theoretically to be a weakly bound dimer of NO.^{21–24}

The aforementioned channels have been carefully considered in our calculations. Optimized geometries of various stable species and transition states are shown in Figures 1 and 2, respectively. Their energies are presented in Table 1.

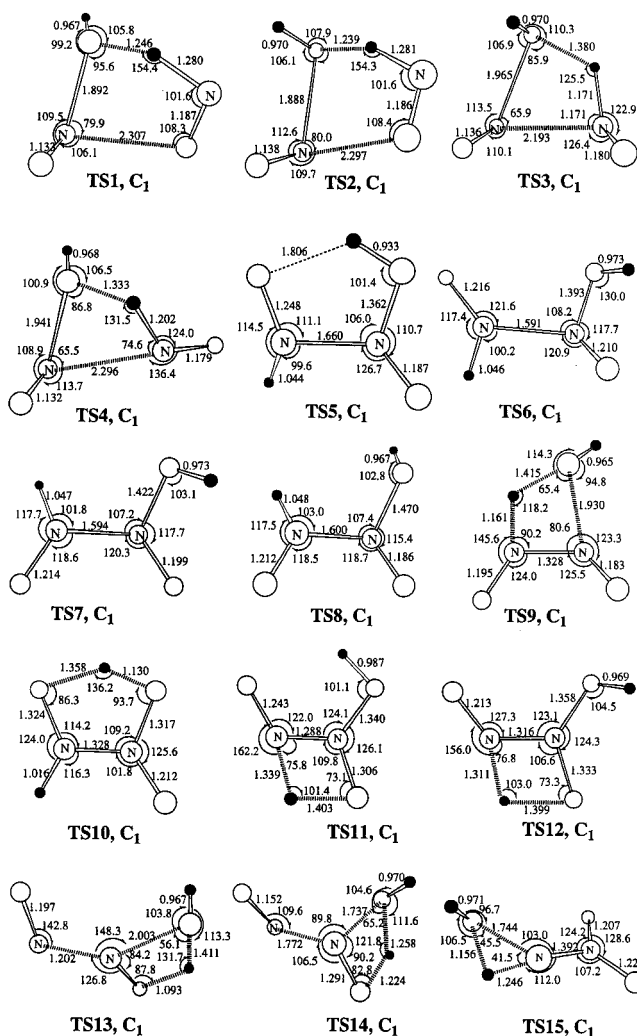


Figure 2. B3LYP/6-311G(d,p) optimized structures (bond lengths in angstroms, bond angles in degrees) of transition states of the HNO + HONO reaction.

Hydrogen-Bonding Complexes of HNO and HONO. HNO and HONO are polar molecules that are prone to form hydrogen-bonding $[\text{ONH} \cdots \text{O}(\text{H})\text{NO}]$ complexes. Our recent IRC//B3LYP/6-311G(d,p) study of the bimolecular decomposition of HONO ²⁵ reveals that some H-bonding complexes of the reactants work as precursors for the direct H-abstraction process (i.e., the direct elimination of H_2O) in the HONO + HONO reaction system. For the present (HNO–HONO) system, we have found six H-bonding complexes in the potential energy surface. These are **H1**–**H6** shown in Figure 1. The predicted binding energies of these complexes range from 0.8 to 3.5 kcal/mol (Table 1) at the G2M level of theory. Among these complexes, the planar, seven-member ringlike complex, **H1**, which is formed by $\text{cis-HONO} + \text{HNO}$, is the most stable. According to the structural features of these hydrogen-bonding complexes, it can be inferred that the complexes **H3**, **H4**, **H5**, and **H6** may be the precursors of the direct elimination of H_2O between HNO and HONO.

Direct Elimination of H_2O . The final products of this reaction channel are H_2O and 2NO molecules. The reaction is predicted to be exothermic at all levels of theories used. The G2M-predicted exothermicity is 21.0 kcal/mol. Four transition states corresponding to the direct elimination of H_2O have been located. They are labeled as **TS1**, **TS2**, **TS3**, and **TS4** in Figure 2. **TS1** and **TS4** come from HNO + trans-HONO , and **TS2** and **TS3** are from HNO + cis-HONO . At the G2M level of theory, the barrier heights of these four transition states with

TABLE 1: Energetics^a of Reactants, Products, Intermediates, and Transition States of the HNO+HONO System Calculated at Different Levels of Theory

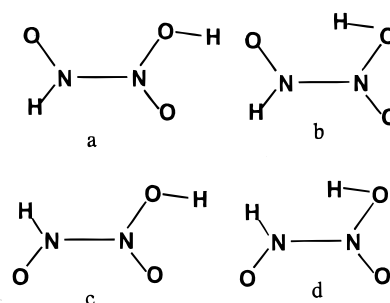
	ZPE ^b	B3LYP/ 6-311G(d,p)	MP2/ 6-311G(d,p)	CCSD(T)/ 6-311G(d,p)	QCISD(T)/ 6-311G(d,p)	MP2/ 6-311G(3df,2p)	G2M(RCC,MP2)
<i>trans</i> -HONO+HNO	21.4	-336.27068 ^c	-335.46705 ^c	-335.51798 ^c	-335.52030 ^c	-335.67572 ^c	-335.77410 ^c
<i>cis</i> -HONO+HNO	21.4	-336.27106 ^c	-335.46777 ^c	-335.51854 ^c	-335.52072 ^c	-335.67513 ^c	-335.77340 ^c
H1	23.6	-0.2	-0.5	-0.4	-0.3	+0.4	+0.4
H2	23.5	-5.4	-4.9	-4.8	-4.7	-3.5	-3.5
H3	23.2	-4.6	-4.6	-4.3	-4.3	-3.8	-1.4
H4	23.2	-3.9	-3.9	-3.7	-3.7	-2.9	-2.7
H5	23.0	-3.5	-3.8	-3.5	-3.4	-0.8	-2.1
H6	22.6	-2.5	-3.0	-2.8	-2.8	-2.2	-2.0
H6	22.6	-2.1	-2.5	-2.2	-2.2	-1.1	-0.8
TS1	20.7	+8.8	+18.6	+19.7	+18.1	+19.6	+20.6
TS2	20.6	+10.2	+20.5	+20.9	+19.5	+21.6	+21.9
TS3	20.6	+18.9	+27.7	+31.1	+29.3	+27.3	+30.6
TS4	20.5	+17.2	+27.2	+29.4	+29.2	+27.6	+29.7
TS5	24.7	+13.8	+25.3	+26.2	+24.7	+20.8	+21.7
TS6	24.5	+18.1	+25.9	+29.5	+28.4	+21.7	+25.4
TS7	24.4	+16.1	+23.3	+27.3	+26.3	+19.1	+23.1
TS8	24.1	+19.7	+27.0	+30.8	+29.7	+22.3	+26.0
TS9	21.8	+34.2	+44.1	+46.0	+44.6	+39.4	+41.2
TS10	21.2	+2.6	+7.3	+15.8	+15.6	+0.2	+11.6
TS11	22.8	+41.6	+43.5	+52.6	+52.4	+36.0	+43.1
TS12	22.6	+43.6	+47.8	+54.5	+54.1	+41.5	+48.1
TS13	21.9	+35.0	+28.1	+46.4	+45.8	+20.8	+39.1
TS14	20.5	+39.4	+43.2	+43.9	+43.7	+40.0	+38.0
TS15	22.3	+42.3	+47.2	+52.6	+51.9	+43.8	+49.2
NN1	26.3	+11.1	+14.3	+23.9	+23.9	+6.0	+15.5
NN2	26.2	+5.3	+9.7	+18.5	+18.4	+1.0	+9.9
NN3	25.9	+10.9	+13.6	+24.0	+24.0	+5.0	+15.4
NN4	27.1	-12.0	+0.7	+9.0	+9.1	-5.7	+2.7
NN5	25.4	+0.4	+5.0	+6.8	+6.9	+1.2	+3.0
NN6	24.9	+2.1	+5.3	+6.5	+6.7	+2.8	+3.9
NN(O)O+H ₂ O	21.1	+26.8	+29.5	+29.7	+29.9	+28.4	+31.8
<i>trans</i> -(NO) ₂ +H ₂ O	20.6	-12.5	-15.7	-16.4	-15.8	-17.0	-18.3
<i>cis</i> -(NO) ₂ +H ₂ O	21.1	-16.9	-24.8	-20.0	-21.0	-21.1	-23.3
2NO+H ₂ O	19.1	-21.3	-22.9	-26.8	-26.4	-20.1	-21.0

^a Relative energies in kcal/mol with respect to *trans*-HONO + HNO. ^b Zero-point energy corrections (kcal/mol), calculated at the B3LYP/6-311G(d,p) level. ^c Total energies are given in hartrees.

respect to the corresponding free reactants are 20.6, 21.5, 30.2, and 29.7 kcal/mol, respectively. IRC//B3LYP/6-311 G(d,p) calculations reveal that **TS1**, **TS2**, **TS3**, and **TS4** actually derive from the 4 H-bonding complexes, that is, **H5**, **H6**, **H4**, and **H3**, respectively. This confirms the inference made in the preceding paragraph. The IRC calculations also indicate that both **TS1** and **TS2** lead to the direct products of H₂O + 2NO, whereas **TS3** and **TS4** result in the formation of *cis*-N₂O₂ and *trans*-N₂O₂ intermediates, respectively. It is known that *trans*-N₂O₂ is unstable, and *cis*-N₂O₂ is very weakly bound with a dimerization energy of 2–4 kcal/mol (experimental value^{21,22}). Our G2M calculations predict a metastable *trans*-N₂O₂, and a dimerization energy of 2.3 kcal/mol for *cis*-N₂O₂, in good accordance with the experimental observations.

Association–Elimination Mechanism. Topologically there should exist four isomers of N–N bonding HN(O)N(O)OH formed by the association of HNO with *cis*- and *trans*-HONO, as depicted in Scheme 1. However, only three conformers have been found in the potential energy surface (PES) of HN(O)N(O)OH. They are **NN1**, **NN2**, and **NN3** in Figure 1, corresponding to (a), (b), and (c) in the scheme. Optimization with an initial geometry like that given in Scheme 1 (c) or (d) converges to a common, nonplanar conformer, **NN3**. All three conformers are formed endothermically with respect to free HNO and HONO. Among these conformers, **NN2** is the lowest in energy because of the existence of intramolecular hydrogen bonding. Note that the distance between the O atom of the HNO group and the H atom of the HONO group in **NN2** is only 1.773 Å, even shorter

SCHEME 1



than the shortest H-bonding distance in the H-bonding [ONH–O(H)NO] complexes (1.890 Å in **H1**).

Four transition states that connect the HN(O)N(O)OH conformers and the reactants are shown in Figure 2. **TS5** leads to the formation of **NN2** from HNO + *trans*-HONO. **TS6** leads to the formation of **NN1** from HNO + *cis*-HONO. Both **TS7** and **TS8**, which derive from *cis*- and *trans*-HONO reactions, respectively, result in **NN3**. At the G2M level of theory, the barrier heights for **TS5**–**TS8** are, respectively, 21.7, 25.0, 22.7, and 26.0 kcal/mol; these values are comparable with those for direct elimination of H₂O.

Among the three conformers of HN(O)N(O)OH, only **NN3** can eliminate H₂O by reaction 2, whereas for **NN1** and **NN2**, intramolecular H-transfer is required to reach a geometry that can undergo further dehydration. The dehydration of **NN3** proceeds by transition state, **TS9**, which is higher than **NN3** by

TABLE 2: Molecular and Transition-State Parameters of the Reactants, and Transition States of the HNO + HONO and NH₃ + HONO Reactions, Used for TST Calculations of Rate Constants [Calculated at the B3LYP/6-311G(d,p) Level]

species	I_f (10 ⁻¹⁴ g cm ²)	frequencies (cm ⁻¹)
<i>trans</i> -HONO	8.9, 67.4, 76.3	591, 618, 834, 1298, 1793, 3776
<i>cis</i> -HONO	10.1, 63.2, 73.4	638, 719, 892, 1338, 1721, 3584
HNO	1.5, 19.7, 21.2	1577, 1674, 2828
NH ₃	2.9, 2.9, 4.5	1069, 1681, 1682, 3464, 3583, 3583
HNO + HONO reaction		
TS1	107.3, 218.5, 300.2	1234i, 132, 198, 350, 380, 400, 568, 630, 663, 784, 1332, 1612, 1711, 1939, 3796
TS2	119.0, 223.4, 306.2	1229i, 129, 191, 340, 386, 391, 585, 637, 659, 796, 1291, 1627, 1720, 1911, 3752
NH ₃ + HONO reaction		
TS1'	95.7, 124.1, 197.3	1231i, 271, 294, 343, 450, 458, 620, 640, 646, 755, 793, 1480, 1666, 1702, 1905, 3505, 3627, 3816
TS2'	96.0, 125.3, 198.8	1227i, 267, 271, 335, 454, 490, 603, 643, 665, 777, 792, 1477, 1670, 1703, 1873, 3504, 3626, 3790
TS8'	66.4, 148.4, 210.1	465i, 220, 342, 363, 405, 504, 827, 1043, 1310, 1326, 1482, 1604, 1625, 1687, 2312, 2664, 3492, 3585

TABLE 3: Fitted Expressions for Rate Constants^a (cm³ mol⁻¹ s⁻¹) and Apparent Activation Energies (kcal/mol) of the HNO + HONO Reactions

reaction	300–3000 K 3-parameter fitting	300 K	300–1000 K 2-parameter fitting	E_a
<i>trans</i> -HONO + HNO, k_1	$1.72 \times 10^{-3} T^{4.13} \exp(-8350/T)$	3.01×10^{-5}	$2.55 \times 10^{10} \exp(-10500/T)$	20.9
<i>cis</i> -HONO + HNO, k_2	$1.76 \times 10^{-3} T^{4.18} \exp(-8850/T)$	7.86×10^{-6}	$3.63 \times 10^{10} \exp(-11000/T)$	21.9

^a Eckart tunneling correction was used to compute the rate constants (see ref 27).

25.8 kcal/mol and higher than the HNO + *trans*-HONO reactants by 41.4 kcal/mol at the G2M level. For NN2, H-transfer may proceed from HONO to HNO via TS10 to the intermediate NN4 or from HNO to HONO via TS11 to NN5. The barrier height for the former process is very low (1.7 kcal/mol), whereas for the latter the barrier height is very high, 33.2 kcal/mol. The reactions from free HNO + *trans*-HONO to NN4 and NN5 are nearly thermoneutral, 2.7 kcal/mol for the former and 3.0 kcal/mol for the latter. For NN1, the H-transfer from HNO to HONO via TS12 results in the intermediate NN6, which is only ~1.0 kcal/mol higher than NN4 and NN5. This H-transfer process has a barrier height of 22.6 kcal/mol, but TS12 is higher than the reactants by 48.1 kcal/mol. NN4, NN5, and NN6 are ready for further dehydration, as suggested by their geometries.

The dehydration of NN4 gives rise to N=N(O)O, which is a high-energy isomer of N₂O₂. This process goes through a transition state, TS15, with a barrier height (46.5 kcal/mol) too high to be important; it is also highly endothermic. The dehydration of NN5 proceeds via a transition state, TS13, with a barrier height of 36.1 kcal/mol, resulting in the formation of *trans*-N₂O₂. The dehydration of NN6 also produces *trans*-N₂O₂. The corresponding transition state TS14 has a barrier height of 34.1 kcal/mol.

All the aforementioned reaction channels are schematically shown in Figure 3. Clearly, for the reduction of HONO by HNO via HN(O)N(O)OH, it has to pass through transition states with very high barriers for the dehydration process. Accordingly, the association/elimination reaction involving HN(O)N(O)OH intermediates cannot compete effectively with the direct dehydration processes described above.

TST Calculations of Rate Constants. We have shown in our ab initio MO calculations that the key channels responsible for the HNO + HONO are those taking place by direct elimination of H₂O via hydrogen-bonding complexes. These are the reactions that go through TS1–TS4. As the barrier heights of TS3 and TS4 are higher than those of TS1 and TS2 by about 9–10 kcal/mol, we only consider the channels occurring via TS1 and TS2 in our rate constant calculations using TST.²⁶ The barrier heights calculated at the G2M level (given in Table 1) and the B3LYP/6-311G(d,p) molecular parameters of the reactants and transition states (Table 2) were used in our TST calculations. A complete summary of molecular parameters is presented in

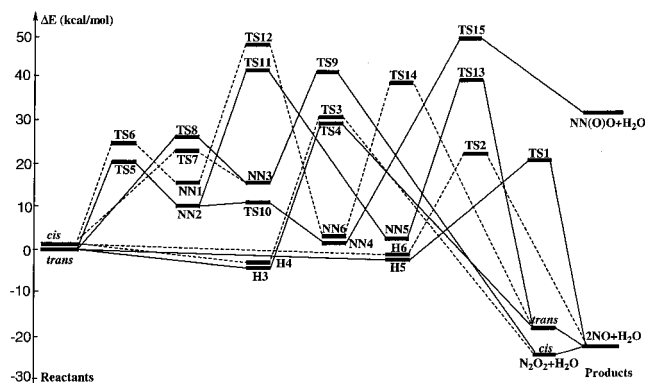


Figure 3. Energy diagram for the potential energy surface of the HNO + HONO reaction calculated in the framework of the G2M(RCC, MP2)/B3LYP/6-311G(d,p) approach. Solid lines connect the *trans*-HONO related channels; dotted lines connect the *cis*-HONO related channels.

Appendix A. We used the conventional TST method with Eckart tunneling corrections described earlier.²⁷ The rate constant expressions obtained by 2- and 3-parameter fitting are presented in Table 3. For the reaction HNO + *trans*-HONO → TS1 → 2NO + H₂O, 2-parameter fitting in the 300–1000 K temperature range gives an A factor of 2.55×10^{10} cm³ mol⁻¹ s⁻¹ and an apparent activation energy of 20.9 kcal/mol. The reaction HNO + *cis*-HONO → TS2 → 2NO + H₂O is slightly slower, with an A factor of 3.63×10^{10} cm³ mol⁻¹ s⁻¹ and an apparent activation energy of 21.9 kcal/mol.

HONO + NH₃ Reaction. For the NH₃ + HONO reaction, the experimental work of Kaiser and Japar gave an upper limit for the rate constant ($\leq 9.04 \times 10^6$ cm³ mol⁻¹ s⁻¹),²⁸ which is at least 4 orders slower than the NH₃ + HNO₃ reaction. Unfortunately, the products of the reaction were not clearly identified in their paper. The recent ab initio study of the bimolecular reaction of NH₃ with HNO₃ suggested the following two major channels,²⁹



and predicted that both channels have approximately the same barrier, 46 kcal/mol. We expect that a similar mechanism may

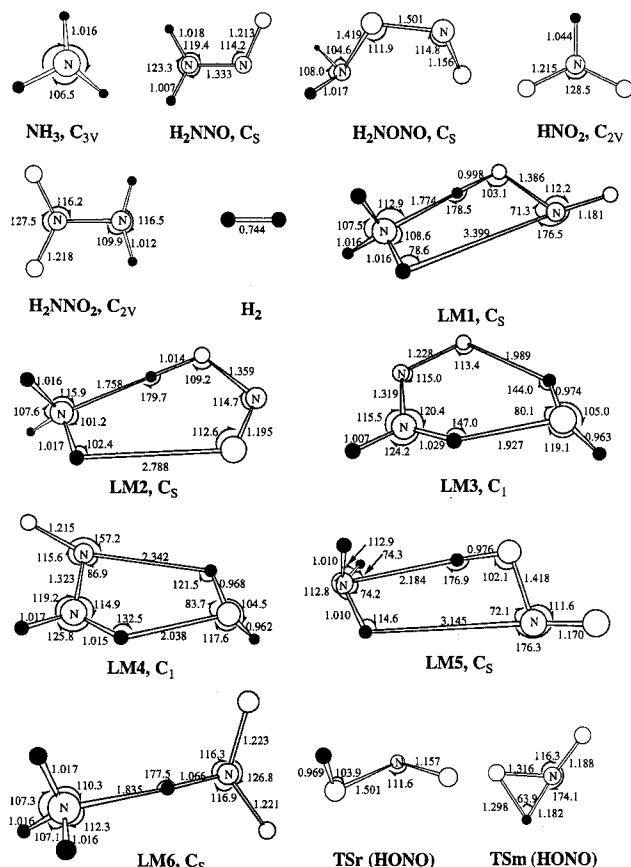


Figure 4. B3LYP/6-311G(d,p) optimized structures (bond lengths in angstroms, bond angles in degrees) of NH₃, intermediates, and products of the NH₃ + HONO reaction.

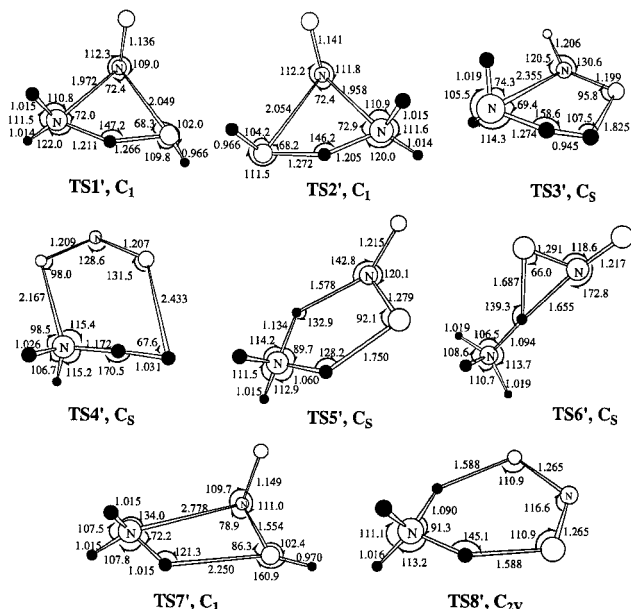


Figure 5. B3LYP/6-311G(d,p) optimized structures (bond lengths in angstroms, bond angles in degrees) of transition states of the NH₃ + HONO reaction.

exist in the NH₃ + HONO reaction system, viz.



Another possible reaction may take place by H₂ elimination,



TABLE 4: Energetics^a of Reactants, Intermediates, and Transition States of the NH₃ + HONO System Calculated at Different Levels of Theory

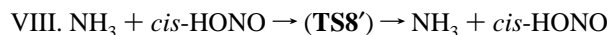
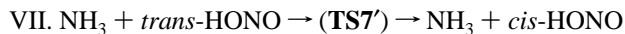
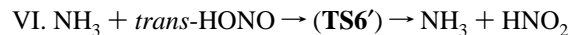
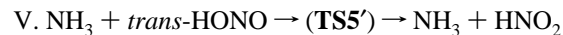
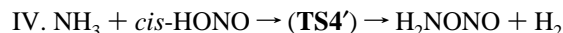
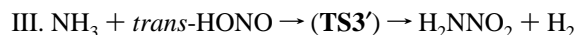
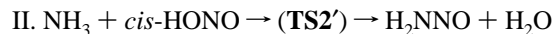
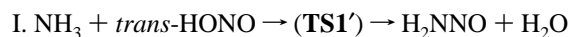
species	ZPE ^b	B3LYP/ 6-311G(d,p)	G2M (RCC,MP2)
NH ₃ + <i>trans</i> -HONO	34.2	-262.33780 ^c	-261.91684 ^c
NH ₃ + <i>cis</i> -HONO	34.2	-262.33819 ^c	-261.91613 ^c
		(-0.2)	(+0.4)
TS1'	32.8	24.6	33.4
TS2'	32.8	26.0	34.9
TS3'	29.7	97.4	101.6
TS4'	28.2	92.9	97.7
TS5'	35.8	11.0	15.4
TS6'	36.0	21.3	21.3
TS7'	34.2	9.6	9.3
TS8'	35.4	0.3	5.9
LM1	36.5	-11.5	-8.2
LM2	36.3	-11.4	-7.1
LM3	36.7	-17.5	-13.8
LM4	36.2	-15.7	-12.8
LM5	35.5	-2.6	-0.2
LM6	37.2	-4.1	-0.0
H ₂ NNO + H ₂	29.1	46.5	49.5
H ₂ NNO ₂ + H ₂	30.9	23.8	29.7
NH ₃ + HNO ₂	35.3	7.3	8.7
H ₂ NNO + H ₂ O	35.5	-8.8	-7.1

^a Relative energies in kcal/mol with respect to NH₃ + *trans*-HONO.

^b Zero-point energy corrections (kcal/mol), calculated at the B3LYP/6-311G(d,p) level. ^c Total energies are given in hartrees.

These reactions as well as the other possibilities have been carefully considered in our calculations. Optimized geometries of various species and stationary points for the NH₃ + HONO reaction are shown in Figures 4 and 5. The total energy of the reactants and the relative energies of the transition states, intermediates, and products calculated at the B3LYP/6-311G(d,p) and G2M(RCC, MP2) level of theory, as well as the values of ZPE corrections are summarized in Table 4. The schematic energy diagram for the potential energy surface of the reaction under consideration is illustrated in Figure 6.

Potential Energy Surface. Our B3LYP//IRC//G2M calculations for the reaction of ammonia with nitrous acid reveal eight possible distinct pathways (I–VIII) that lead to the formation of four different sets of final products, H₂NNO + H₂O, H₂NNO₂ + H₂, H₂NONO + H₂, and NH₃ + HNO₂. They are



Let us consider these channels in detail. As can be seen from the PES presented in Figure 6, the channel I, NH₃ + *trans*-HONO → LM1 → TS1' → LM3 → H₂NNO + H₂O, proceeds by abstraction of a hydrogen atom from NH₃ by the O(H) atom of *trans*-HONO, followed by breaking the O(H)–N bond of HONO and the association of H₂N with NO. This reaction is exothermic by 7.1 kcal/mol and has an activation barrier of 33.4 kcal/mol. Interestingly, the hydrogen-bonding intermediate,

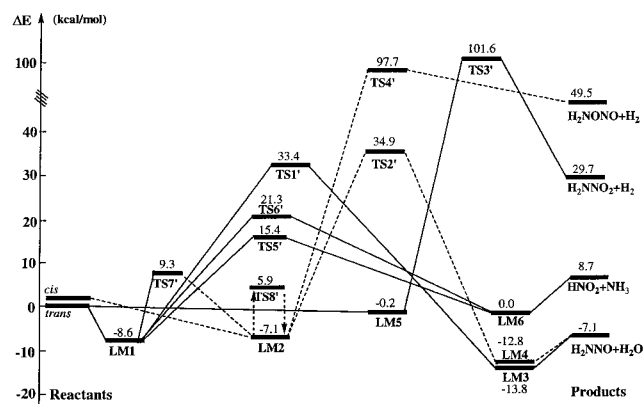


Figure 6. Energy diagram for the potential energy surface of the $\text{NH}_3 + \text{HONO}$ reaction calculated in the framework of the G2M(RCC,-MP2)//B3LYP/6-311G(d,p) approach. Solid lines connect the *trans*-HONO related channels; dotted lines connect the *cis*-HONO related channels.

LM1, has been found to work as a precursor of the H-abstraction transition state, **TS1'**. Following **TS1'** in the reaction path, there exists another intermediate, **LM3**, which is a H-bonding complex of the products, $\text{H}_2\text{NNO} + \text{H}_2\text{O}$. With $\text{NH}_3 + \text{cis-HONO}$ as the reactants, we have a similar channel (**II**), $\text{NH}_3 + \text{cis-HONO} \rightarrow \text{LM2} \rightarrow \text{TS2'} \rightarrow \text{LM4} \rightarrow \text{H}_2\text{NNO} + \text{H}_2\text{O}$, which is exothermic by 7.5 kcal/mol. The barrier height was found to be 34.5 kcal/mol, slightly higher than that of channel **I**. The intermediates, **LM2** and **LM4**, in this channel are H-bonding complexes of the reactants and the products, respectively. **LM4** has a five-member ring structure with hydrogen-bonding involving $\text{H}\cdots\text{O}$ and $\text{H}\cdots\text{N}$, whereas **LM3** of channel **I** has a six-member ring structure with two $\text{H}\cdots\text{O}$ bonds. The hydrogen-bonding interaction between H_2O and H_2NNO in **LM3** is stronger than that in **LM4**, as indicated by the lower total energy of **LM3** and the shorter $\text{H}\cdots\text{O}$ bond lengths in **LM3**. Channel **III**, $\text{NH}_3 + \text{trans-HONO} \rightarrow \text{LM5} \rightarrow \text{TS3'} \rightarrow \text{H}_2\text{NNO}_2 + \text{H}_2$, goes through a van der Waals intermediate **LM5** and transition state, **TS3'**. A similar channel, **IV**, that involves *cis*-HONO via the intermediate **LM2** and transition state **TS4'**, however, leads to a different product, H_2NONO . Both channels **III** and **IV** are not expected to be practically important in the $\text{NH}_3 + \text{HONO}$ reaction, because they are sufficiently endothermic and require much higher activation energies (101.6 kcal/mol for channel **III** versus 97.3 kcal/mol for channel **IV**). Reaction channels **V**, $\text{NH}_3 + \text{trans-HONO} \rightarrow \text{LM1} \rightarrow \text{TS5'} \rightarrow \text{LM6} \rightarrow \text{HNO}_2 + \text{NH}_3$, and **VI**, $\text{NH}_3 + \text{trans-HONO} \rightarrow \text{LM1} \rightarrow \text{TS6'} \rightarrow \text{LM6} \rightarrow \text{HNO}_2 + \text{NH}_3$, are endothermic by 8.6 kcal/mol; they lead to the formation of HNO_2 and NH_3 products via transition states **TS5'** and **TS6'**, respectively. The barrier heights of channels **V** and **VI** are 15.4 and 21.3 kcal/mol, respectively. It is worth noting that both reaction channels have a common prereaction intermediate (**LM1**), a common postreaction intermediate (**LM6**), and common products. However, channel **V** involves H-atom exchange between NH_3 and *trans*-HONO, whereas channel **VI** is an NH_3 -catalyzed intramolecular H-transfer process within HONO. A similar unimolecular isomerization process, *trans*-HONO \rightarrow HNO_2 , occurs via transition state, **TSm** (see Figure 4), with an activation energy of 55.2 kcal/mol (see Figure 7). [This G2M prediction is in good agreement with the previous prediction of 55.2 kcal/mol obtained by Jursic³⁰ at the B3LYP/6-311G(3df, 3dp) level of theory.] Hence, the presence of NH_3 promotes the isomerization of *trans*-HONO into HNO_2 by reducing the energy barrier by as much as 34 kcal/mol. Reaction channel **VII**, $\text{NH}_3 + \text{trans-HONO} \rightarrow \text{LM1} \rightarrow \text{TS7'} \rightarrow \text{LM2} \rightarrow \text{NH}_3 + \text{cis-HONO}$, corresponds to the *trans*-*cis*

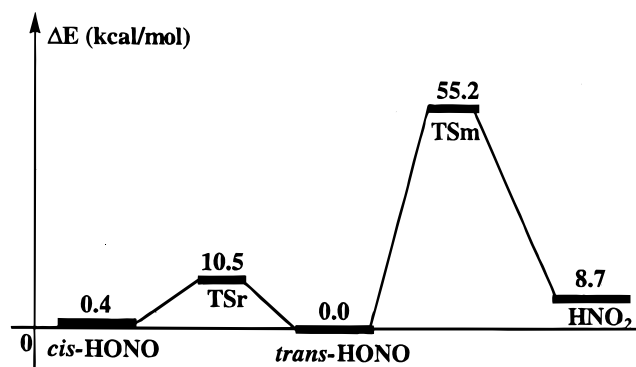


Figure 7. Energy diagram for the potential energy surface of the isomerization of an isolated HONO calculated in the framework of the G2M(RCC,MP2)//B3LYP/6-311G(d,p) approach.

isomerization of HONO in the presence of NH_3 . Indeed, the transition state, **TS7'**, is simply a H-bonding complex of NH_3 with the rotational transition state (**TSr**) for the *trans*-*cis* isomerization of HONO. The barrier height of this channel is 9.3 kcal/mol with respect to free $\text{NH}_3 + \text{trans-HONO}$, and 17.9 kcal/mol with respect to **LM1**. For the *trans*-*cis* isomerization of an isolated HONO molecule, our G2M calculations predict a rotational transition state, **TSr** (see Figure 4), which is higher than *trans*-HONO by 10.5 kcal/mol (see Figure 7). It is clear that the presence of NH_3 somewhat hinders the *trans*-*cis* isomerization of HONO. Besides the aforementioned transition states (**TS1'**–**TS7'**), we also located a transition state, **TS8'**, that connects the two equivalent isomers of **LM2** in the potential energy surface of the ($\text{NH}_3 + \text{cis-HONO}$) system. This reaction path, channel **VIII**, describes a reversible gas-phase reaction $\text{NH}_3 + \text{cis-HONO} \rightleftharpoons \text{NH}_2\text{H} + \text{cis-HONO}$, which was studied experimentally by infrared diode laser spectroscopy.³¹ The activation energy of this reversible exchange reaction predicted at the G2M level of theory is only 5.5 kcal/mol.

Calculation of Rate Constants. The rate constants for the $\text{NH}_3 + \text{trans-HONO}$ reaction via **TS1'** (channel **I**) and for the $\text{NH}_3 + \text{cis-HONO}$ reaction via **TS2'** (channel **II**) have been calculated by TST with Eckart tunneling corrections, using the activation barriers and molecular parameters given in Tables 4 and 2, respectively. A complete summary of the molecular parameters for the system is presented in Appendix B. Two-parameter fitting in the 300–1000 K temperature range gives the following Arrhenius expressions (in $\text{cm}^3 \text{mol}^{-1} \text{s}^{-1}$) for channels **I** and **II**:

$$k_{\text{I}} = 3.16 \times 10^{10} \exp(-16800/T)$$

$$k_{\text{II}} = 4.06 \times 10^{10} \exp(-17400/T)$$

with the corresponding apparent activation energies of 33.3 and 34.5 kcal/mol, respectively. The 3-parameter expressions also in $\text{cm}^3 \text{mol}^{-1} \text{s}^{-1}$ fitted in the temperature range 300–3000 K are:

$$k_{\text{I}} = 9.64 \times 10^{-4} T^{4.24} \exp(-14600/T)$$

$$k_{\text{II}} = 1.08 \times 10^{-3} T^{4.26} \exp(-15200/T)$$

At 300 K, the calculated rate constants for the two channels are 3.36×10^{-14} and $5.62 \times 10^{-15} \text{ cm}^3 \text{mol}^{-1} \text{s}^{-1}$, respectively, which are significantly lower than the upper limit reported by Kaiser and Japar,²⁸ $9 \times 10^6 \text{ cm}^3 \text{mol}^{-1} \text{s}^{-1}$. We have performed TST calculations for channel **VIII**, which has the lowest barrier

height. The calculated rate constant for this reversible exchange reaction at 300K is $1.06 \times 10^6 \text{ cm}^3 \text{ mol}^{-1} \text{ s}^{-1}$, in good accordance with the experimental value of $2.2 \times 10^6 \text{ cm}^3 \text{ mol}^{-1} \text{ s}^{-1}$. Two-parameter fitting in the 300–1000 K temperature range gives the rate constant expression, $k_{\text{VIII}} = 1.42 \times 10^{10} \exp(-2930/T) \text{ cm}^3 \text{ mol}^{-1} \text{ s}^{-1}$, with the apparent activation energy of 5.8 kcal/mol.

IV. Concluding Remarks

The gas-phase reactions of HONO with HNO and NH₃ have been investigated using ab initio MO and TST calculations. The

main reaction channels for the HNO + *trans*-HONO and HNO + *cis*-HONO reactions are those proceeding via five-membering transition states, leading to the elimination of H₂O. The corresponding barrier heights center around 21 kcal/mol. The reaction is exothermic by 21 kcal/mol. TST calculations with tunneling corrections gave the rate constants $k_1 = 1.72 \times 10^{-3} T^{4.13} \exp(-8350/T)$ and $k_2 = 1.76 \times 10^{-3} T^{4.18} \exp(-8850/T) \text{ cm}^3 \text{ mol}^{-1} \text{ s}^{-1}$ for the two reaction channels, respectively. Other channels that go through the HN(O)N(O)OH intermediates have been shown to require much higher activation energies for further dehydration and, therefore, are unfavorable.

Appendix A: Overall Moments of Inertia (10^{-40} g cm^2), and Vibrational Frequencies (cm^{-1}) for Various Species Involved in the HONO + HNO Reaction Computed at B3LYP/6-311G(d,p)

species	I _a , I _b , I _c	frequencies
<i>trans</i> -HONO	8.9, 67.4, 76.3	591, 618, 834, 1298, 1793, 3776
<i>cis</i> -HONO	10.1, 63.2, 73.4	638, 719, 892, 1338, 1721, 3584
HNO	1.5, 19.7, 21.2	1577, 1674, 2828
H1	81.5, 308.5, 390.0	83, 147, 166, 179, 244, 460, 701, 901, 981, 1423, 1591, 1670, 1677, 2979, 3331
H2	65.2, 381.3, 446.5	89, 103, 141, 165, 221, 385, 675, 787, 893, 1409, 1595, 1675, 1772, 2961, 3596
H3	42.3, 489.6, 498.5	41, 82, 107, 148, 236, 390, 636, 783, 847, 1355, 1592, 1672, 1790, 2921, 3615
H4	58.5, 431.0, 470.6	31, 82, 110, 162, 238, 361, 636, 823, 896, 1360, 1593, 1672, 1724, 2918, 3472
H5	92.4, 314.1, 352.6	46, 51, 75, 150, 179, 276, 578, 607, 805, 1283, 1593, 1675, 1800, 2921, 3772
H6	77.9, 337.6, 398.6	53, 64, 119, 132, 192, 324, 576, 690, 839, 1308, 1589, 1679, 1746, 2925, 3605
TS1	107.3, 218.5, 300.2	1234i, 132, 198, 350, 380, 400, 568, 630, 663, 784, 1332, 1612, 1711, 1939, 3796
TS2	119.0, 223.4, 306.2	1229i, 129, 191, 340, 386, 391, 585, 637, 659, 796, 1291, 1627, 1720, 1911, 3752
TS3	118.3, 225.7, 309.5	1225i, 39, 190, 270, 349, 438, 535, 569, 656, 733, 1364, 1726, 1888, 1921, 3750
TS4	95.8, 284.6, 357.3	1352i, 99, 158, 233, 341, 429, 524, 559, 662, 756, 1320, 1730, 1763, 1951, 3791
TS5	73.2, 194.9, 264.6	399i, 205, 268, 455, 591, 694, 725, 864, 1077, 1347, 1417, 1476, 1702, 3121, 3328
TS6	76.7, 199.9, 272.2	478i, 194, 277, 389, 518, 577, 625, 825, 1078, 1345, 1463, 1513, 1580, 3095, 3686
TS7	77.2, 207.9, 278.1	430i, 143, 191, 294, 488, 537, 612, 868, 958, 1260, 1447, 1538, 1649, 3063, 3780
TS8	75.2, 207.1, 276.7	428i, 180, 274, 358, 514, 563, 588, 898, 985, 1336, 1451, 1535, 1615, 3090, 3687
TS9	113.0, 177.2, 280.7	1376i, 158, 234, 275, 452, 555, 590, 638, 841, 931, 1217, 1643, 1678, 2212, 3825
TS10	67.8, 166.9, 234.3	1023i, 293, 425, 545, 623, 774, 814, 1010, 1053, 1189, 1343, 1456, 1634, 2188, 3549
TS11	84.4, 161.5, 246.0	1839i, 277, 260, 396, 494, 545, 828, 950, 1030, 1230, 1384, 1513, 1598, 2099, 3479
TS12	87.5, 169.5, 254.5	1813i, 177, 197, 294, 357, 547, 810, 898, 1076, 1192, 1299, 1460, 1609, 2120, 3741
TS13	73.5, 262.0, 332.9	1078i, 160, 199, 371, 466, 481, 590, 702, 772, 1142, 1194, 1344, 1867, 2259, 3794
TS14	84.5, 222.1, 276.7	1031i, 75, 223, 285, 300, 451, 522, 724, 759, 934, 1205, 1307, 1857, 1951, 3772
TS15	71.1, 201.6, 269.3	1590i, 152, 255, 404, 432, 590, 692, 769, 916, 1005, 1326, 1370, 1652, 2285, 3760
NN1	75.3, 176.5, 251.8	276, 324, 341, 399, 529, 702, 714, 853, 1249, 1326, 1395, 1523, 1677, 3363, 3744
NN2	72.2, 170.3, 242.5	282, 342, 442, 551, 573, 694, 759, 881, 1176, 1335, 1373, 1519, 1699, 3242, 3470
NN3	74.9, 183.7, 258.2	194, 245, 317, 350, 496, 639, 662, 982, 1119, 1299, 1419, 1585, 1683, 3377, 3756
NN4	72.5, 183.4, 248.3	174, 297, 380, 510, 614, 774, 835, 1024, 1097, 1362, 1383, 1503, 1723, 3510, 3798
NN5	78.4, 171.4, 241.9	213, 350, 379, 431, 488, 508, 699, 838, 1088, 1139, 1425, 1446, 1570, 3458, 3375
NN6	83.6, 175.9, 246.8	216, 276, 323, 357, 367, 494, 618, 785, 977, 1075, 1352, 1441, 1692, 3673, 3800
NN(O)O	60.0, 64.1, 124.2	387, 622, 658, 889, 1296, 1557
<i>trans</i> -N ₂ O ₂	14.7, 183.0, 197.7	88, 241, 270, 779, 1775, 1914
<i>cis</i> -N ₂ O ₂	31.9, 123.9, 155.7	249, 304, 404, 713, 1781, 1962
NO	16.4, 16.4	1984
H ₂ O	1.1, 1.9, 3.0	1640, 3819, 3906

Appendix B: Overall Moments of Inertia (10^{-40} g cm^2), and Vibrational Frequencies (cm^{-1}) for Various Species Involved in the NH₃ + HONO Reaction Computed at B3LYP/6-311G(d,p)

species	I _a , I _b , I _c	frequencies
<i>trans</i> -HONO	see Appendix A	
<i>cis</i> -HONO	see Appendix A	
NH ₃	2.9, 2.9, 4.5	1069, 1681, 1682, 3464, 3583, 3583
TS1'	95.7, 124.1, 97.3	1231i, 271, 294, 343, 450, 458, 620, 640, 646, 755, 793, 1480, 1666, 1702, 1905, 3505, 3627, 3816
TS2'	96.0, 125.3, 198.8	1227i, 267, 271, 335, 454, 490, 603, 643, 665, 777, 792, 1477, 1670, 1703, 1873, 3504, 3626, 3790
TS3'	73.6, 153.7, 222.9	1167i, 145, 291, 314, 417, 428, 650, 820, 847, 869, 1211, 1335, 1365, 1576, 1688, 1782, 3460, 3557
TS4'	73.6, 125.6, 194.8	673i, 92, 227, 269, 294, 427, 551, 722, 782, 862, 1156, 1276, 1432, 1556, 1574, 1617, 3399, 3511
TS5'	44.0, 203.8, 243.0	460i, 221, 300, 416, 485, 514, 811, 1006, 1271, 1415, 569, 1600, 1619, 1661, 2095, 2934, 3526, 3612
TS6'	38.0, 239.4, 272.8	772i, 79, 168, 173, 303, 387, 790, 1136, 1313, 1362, 1504, 1550, 1656, 1701, 2454, 3448, 3562, 3562
TS7'	78.9, 196.3, 255.2	559i, 71, 87, 103, 144, 226, 336, 500, 767, 1035, 1062, 1665, 1687, 1836, 3467, 3594, 3596, 3762
TS8'	66.4, 148.4, 210.1	465i, 220, 342, 363, 405, 504, 827, 1043, 1310, 1326, 1482, 1604, 1625, 1687, 2312, 2664, 3492, 3585
LM1	26.5, 315.4, 337.4	41, 86, 137, 247.0, 334, 387, 719, 925, 1054, 1138, 1508, 1673, 1674, 1748, 3190, 3473, 3589, 3592
LM2	63.7, 206.7, 265.9	62, 95, 171, 252, 344, 396, 713, 1005, 1107, 1130, 1485, 1656, 1677, 1679, 2952, 3468, 3586, 3591
LM3	68.0, 182.8, 248.2	164, 185, 218, 274, 348, 502, 662, 706, 867, 1160, 1278, 1562, 1625, 1660, 3276, 3625, 3677, 3866
LM4	40.6, 267.1, 305.5	103, 122, 203, 227, 264, 487, 520, 647, 815, 1152, 1259, 1573, 1612, 1648, 3426, 3604, 3748, 3876
LM5	29.8, 347.1, 372.2	50, 63, 106, 138, 323, 367, 606, 653, 770, 865, 1375, 1636, 1638, 1779, 3516, 3596, 3677, 3680
LM6	68.3, 241.2, 305.0	23, 45, 197, 213, 385, 433, 790, 1140, 1258, 1391, 1599, 1669, 1675, 1692, 2860, 3471, 3587, 3588
H ₂ NNO	10.3, 65.6, 75.9	187, 631, 723, 1092, 1223, 1580, 1610, 3455, 3697
H ₂ NNO ₂	66.8, 71.1, 136.9	427, 573, 628, 729, 810, 1014, 1240, 1387, 1612, 1687, 3526, 3658
H ₂ NONO	15.9, 173.1, 184.5	191, 259, 377, 499, 760, 1009, 1168, 1337, 1666, 1806, 3452, 3539
HNO ₂	7.8, 64.1, 71.9	801, 1069, 1407, 1542, 1677, 3146
H ₂ O	1.1, 1.9, 3.0	1640, 3810, 3906
H ₂	0.5, 0.5	4419

In the $\text{NH}_3 + \text{HONO}$ system, the reversible exchange reaction $\text{NH}_3 + \text{cis-HONO} \rightleftharpoons \text{H}_2\text{NH}-\text{O}(\text{H})\text{NO} \rightleftharpoons \text{NH}_2\text{H} + \text{cis-HONO}$ has the lowest activation energy, 5.5 kcal/mol. The channels leading to the production of H_2NNO and H_2O require high activation energies (33–35 kcal/mol); they may become important only at high temperatures. A TST calculation predicts the rate constant for the reversible exchange reaction to be $1.06 \times 10^6 \text{ cm}^3 \text{ mol}^{-1} \text{ s}^{-1}$ at 300 K, in good agreement with experimental data.

Acknowledgment. This work was sponsored partially by Emory University and partially by the Caltech Multidisciplinary University Research Initiative under ONR grant no. N00014-95-1388, Program Manager Dr. J. Goldwasser. One of us (X.L.) thanks the Cherry L. Emerson Center for Scientific Computation for financial support.

References and Notes

- (1) Kuo, K. K.; Summerfield, M. *Fundamentals of Solid Propellant Combustion, Progress in Astronautics and Aeronautics*; AIAA: New York, 1984; Vol. 90.
- (2) Alexander, M. H.; Dagdigian, P. J.; Jacox, M. E.; Kolb, C. E.; Melius, C. F.; et al. *Prog. Energy Combust. Sci.* **1991**, 17, 263.
- (3) Adams, G. F.; Shaw, R. W., Jr. *Annu. Rev. Phys. Chem.* **1992**, 43, 311.
- (4) Mebel, A. M.; Lin, M. C.; Morokuma, K.; Melius, C. F. *J. Phys. Chem.* **1995**, 99, 6842.
- (5) Diau, E. W. G.; Lin, M. C.; He, Y.; Melius, C. F. *Prog. Energy Combust. Sci.* **1995**, 21, 1.
- (6) Mebel, A. M.; Lin, M. C.; Morokuma, K. *Int. J. Chem. Kinet.* **1998**, 30, 729.
- (7) Mebel, A. M.; Lin, M. C.; Melius, C. F. *J. Phys. Chem.* **1998**, 102, 1803.
- (8) Lu, X.; Park, J.; Lin, M. C. Manuscript in preparation.
- (9) Becke, A. D. *J. Chem. Phys.* **1992**, 96, 2155.
- (10) Becke, A. D. *J. Chem. Phys.* **1992**, 97, 9173.
- (11) Becke, A. D. *J. Chem. Phys.* **1993**, 98, 5648.
- (12) Lee, C.; Yang, W.; Parr, R. G. *Phys. Rev.* **1988**, B37, 785.
- (13) Hehre, W.; Radom, L.; Schleyer, P. v. R.; Pople, J. A. *Ab Initio Molecular Orbital Theory*; Wiley: New York, 1986.
- (14) Gonzalez, C.; Schlegel, H. B. *J. Chem. Phys.* **1989**, 90, 2154.
- (15) Pople, J. A.; Head-Gordon, M.; Raghavachari, K. *J. Chem. Phys.* **1987**, 87, 5768.
- (16) (a) Purvis, G. D.; Bartlett, R. J. *J. Chem. Phys.* **1982**, 76, 1910. (b) Hampel, C.; Peterson, K. A.; Werner, H.-J. *Chem. Phys. Lett.* **1992**, 190, 1. (c) Knowles, P. J.; Hampel, C.; Werner, H.-J. *J. Chem. Phys.* **1994**, 99, 5219. (d) Deegan, M. J. O.; Knowles, P. J. *Chem. Phys. Lett.* **1994**, 227, 321.
- (17) Mebel, A. M.; Morokuma, K.; Lin, M. C. *J. Chem. Phys.* **1995**, 103, 7414.
- (18) Curtiss, L. A.; Raghavachari, K.; Trucks, G. W.; Pople, J. A. *J. Chem. Phys.* **1991**, 94, 7221.
- (19) Frisch, M. J.; Trucks, G. W.; Schlegel, H. B.; Gill, P. M. W.; Johnson, B. G.; Robb, M. A.; Cheeseman, J. R.; Keith, T.; Petersson, G. A.; Montgomery, J. A.; Raghavachari, K.; Al-Laham, M. A.; Zakrzewski, V. G.; Ortiz, J. V.; Foresman, J. B.; Cioslowski, J.; Stefanov, B. B.; Nanayakkara, A.; Challacombe, M.; Peng, C. Y.; Ayala, P. Y.; Chen, W.; Wong, M. W.; Andres, J. L.; Replogle, E. S.; Gomperts, R.; Martin, R. L.; Fox, D. J.; Binkley, J. S.; Defrees, D. J.; Baker, J.; Stewart, J. P.; Head-Gordon, M.; Gonzalez, C.; Pople, J. A. *Gaussian 94*, revision D.3; Gaussian, Inc.: Pittsburgh, PA, 1995.
- (20) MOLPRO is a package of ab initio programs written by H.-J. Werner and P. J. Knowles, with contributions from J. Almlöf, R. D. Amos, M. J. O. Deegan, S. T. Elbert, C. Hampel, W. Meyer, K. Peterson, R. Pitzer, A. J. Stone, P. R. Taylor, and R. Lindh.
- (21) Menoux, V.; Le Doucen, R.; Haeusler, C.; Deroche, J. C. *Can. J. Phys.* **1984**, 62, 322 and references therein.
- (22) McKellar, A. R.; Watson, J. K. G.; Howard, B. J. *Mol. Phys.* **1995**, 86, 273.
- (23) Lee, T. J.; Rice, J. E.; Scuseria, G. E.; Schaefer, H. F., III. *Theor. Chim. Acta* **1989**, 75, 81.
- (24) Duarte, H. A.; Proynov, E.; Salahub, D. R. *J. Chem. Phys.* **1998**, 109, 26.
- (25) Lu, X. Unpublished results.
- (26) Laidler, K. J. *Chemical Kinetics*, 3rd ed.; Harper and Row: New York, 1987.
- (27) Tokmakov, I. V.; Park, J.; Gheysa, S.; Lin, M. C. *J. Phys. Chem. A* **1999**, 103, 3636.
- (28) Kaiser, E. W.; Japar, S. M. *J. Phys. Chem.* **1978**, 82, 2753.
- (29) Musin, R. N.; Lin, M. C. *J. Phys. Chem. A* **1998**, 102, 1808.
- (30) Jursic, B. S. *Chem. Phys. Lett.* **1999**, 299, 334.
- (31) Pagsberg, P.; Ratajczak, E.; Sillesen, A.; Latajka, Z. *Chem. Phys. Lett.* **1994**, 227, 6.